PABP1 Drives the Selective Translation of Influenza A Virus mRNA

Cyrus M de Rozières, Alberto Pequeno, Shandy Shahabi, Taryn M Lucas,

Kamil Godula, Gourisankar Ghosh and Simpson Joseph*

Department of Chemistry and Biochemistry, University of California, San Diego,

La Jolla, CA 92093-0314, USA

* To whom correspondence should be addressed.

Tel: + 858 822 2957

Fax: + 858 534 7042

Email: sjoseph@ucsd.edu

Supplemental Figure 1. IAV 5'UTR Sequence Conservation of minor population. (A) LOGO analysis of several alternative IAV 5'UTR sections found across segments. For the HA segment 35% and 19% of total UTR sequences analyzed were 29 nt and 28 nt respectively. The alternative NP and M1 segments LOGO made up 19% of total sequences. The NA segment had 6% of sequences with 20 nt and 1% with 21 nt. Analysis is based on DNA sequencing files and thus the RNA would have an uracil instead of a thymine. A black line above the ATG is used to indicate the start codon.

Supplemental Figure 2. RNA-binding specificity of PABP1. (A) The sequences of the RNA used in the binding studies. (B) EMSA assay comparing binding of PABP1 to different control RNA. Minus sign indicates no PABP1 was added to the reaction. Arrow points to the shifted PABP1 monomer•Poly(A)$_{18}$ complex and PABP1 dimer•Poly(A)$_{18}$ complex. (C) Anisotropy assay to analyze the binding of PABP1 to the different control RNAs. The final concentration of the RNAs was 1 nM, and the final concentration of PABP1 was increased from 0 to 5 μM. The change in anisotropy is shown on the y-axis. The error bars represent the standard deviation from three independent experiments. (D) Competition assay to determine the specificity of PABP1 binding to M1-5'-UTR. 1 nM of fluorescently labelled M1-5'-UTR with 250 nM PABP1 was titrated with increasing concentrations of unlabeled M1-5'-UTR. The change in anisotropy is shown on the y-axis. The error bars represent the standard deviation from three independent experiments. (E) Anisotropy assay to analyze the binding of PABP1 to M1-5'-UTR RNA, Poly(A)$_{18}$, and Poly(A)$_{30}$ in the presence or absence of 5 mM Mg^{2+}. The K_Ds are as follows: M1-5'-UTR, 83 nM ± 14 nM and 86 nM ± 7 nM with or without

Mg^{2+} respectively, $Poly(A)_{30}$, 5 nM ± 0.5 nM and 4 nM ± 0.3 nM with or without Mg^{2+} respectively, $Poly(A)_{18}$, 11 nM ± 1 nM and 31 nM ± 4 nM with or without Mg^{2+} respectively. The final concentration of the RNAs was 1 nM, and the final concentration of PABP1 was increased from 0 to 5 μM. The change in anisotropy is shown on the y-axis.

Supplemental Figure 3. PABP1 binds to the 5'UTR of all eight segments of A/Puerto Rico/8/34 (H1N1) IAV. (A) The sequences of the 5'UTRs of A/Puerto Rico/8/34 (H1N1) used in the binding studies. The first guanosine residue is due to T7 transcription and is not part of the native sequence. (B) EMSA assay comparing binding of PABP1 to the different 5'UTR RNA of each IAV segment. Minus sign indicates no PABP1 was added to the reaction. Arrow points to the shifted PABP1 monomer•$Poly(A)_{18}$ complex and PABP1 dimer•$Poly(A)_{18}$ complex. (C) Anisotropy assay to determine the binding affinity of PABP1 for the different 5'UTR RNA of each IAV segment. The final concentration of the RNAs was 1 nM, and the final concentration of PABP1 was increased from 0 to 5 μM. The change in anisotropy is shown on the y-axis. The error bars represent the standard deviation from three independent experiments.

Supplemental Figure 4. PABP1 binds to the 5'UTR of all eight segments of A/Udorn/307/1972 (H3N2) IAV. (A) The sequences of the 5'UTRs of A/Udorn/307/1972 (H3N2) used in the binding studies. The first guanosine residue is due to T7 transcription and is not part of the native sequence. (B) EMSA assay comparing binding of PABP1 to the different 5'UTR RNA of each IAV segment. Minus sign

indicates no PABP1 was added to the reaction. Arrow points to the shifted PABP1 monomer•Poly(A)$_{18}$ complex and PABP1 dimer•Poly(A)$_{18}$ complex. (C) Anisotropy assay to determine the binding affinity of PABP1 for the different 5'UTR RNA of each IAV segment. The final concentration of the RNAs was 1 nM, and the final concentration of PABP1 was increased from 0 to 5 μM. The change in anisotropy is shown on the y-axis. The error bars represent the standard deviation from three independent experiments.

Supplemental Figure 5. Cap-dependent translation inhibition. (A) Translation of Kozak sequence driven *Renilla* luciferase mRNA in HeLa lysate in the presence of increasing amount of m^{7}G cap analog. mRNA is capped at the 5'-end with m^{7}G and have a 25-nucleotide long polyadenosine tail at the 3'-end. Translation was monitored by luminescence and shown as relative luminescence units (RLU). The RLU in the presence of the cap analog was normalized to the control reaction without the cap analog. (B) Translation of Kozak sequence driven *Renilla* luciferase mRNA, M1-5'UTR driven *Renilla* luciferase mRNA, and U2 snRNA + M1-5'UTR driven *Renilla* luciferase mRNA in HeLa lysate. mRNAs are either capped at the 5'-end with m^{7}G and have a 25-nucleotide long polyadenosine tail at the 3'-end (+ Cap/ + Tail) or do not contain an m^{7}G cap and have a 100 nt long random UTR at the 3'-end (- Cap/ - Tail). The RLU of the mRNAs without the cap and tail were normalized to their respective mRNAs with the cap and tail. (C) Translation of nine *Renilla* luciferase mRNAs driven by the different 5'UTR sequence of the 8 segments of A/WSN/1933 (H1N1) IAV in HeLa lysate in the presence or absence of 1 mM m^{7}G cap analog. One-way ANOVA was used to

compare the percent inhibition compared to the Kozak control. The standard deviations from three biological replicates are shown. $P < 0.05$ is denoted with one asterisk, $P < 0.01$ is denoted with two asterisks, $P < 0.001$ is denoted with three asterisks, and $P < 0.0001$ is denoted with four asterisks. (D) Translation of Kozak sequence driven *Firefly* luciferase and CrPV driven *Renilla* luciferase bicistronic mRNA in HeLa lysate in the presence of increasing amount of m^7G cap analog. RNA is capped at the 5'-end with m^7G and has a 25-nucleotide long polyadenosine tail at the 3'-end. The signal for the firefly luciferase in reactions with the cap analog were normalized to the control Kozak driven mRNA translation in the absence of the cap analog. Additionally, the signals for the firefly luciferase were normalized to the *Renilla* luciferase signals for each reaction conditions to normalize for variability. (E) Translation of Kozak, M1-5'UTR, or U2 snRNA + M1-5'UTR sequence driven *Firefly* luciferase and CrPV driven *Renilla* luciferase bicistronic mRNA in HeLa lysate in the presence or absence of 1 mM m^7G cap analog. RNAs are capped at the 5'-end with m^7G and have a 25-nucleotide long polyadenosine tail at the 3'-end. The RLU in the presence of the cap analog was normalized to the control reaction without the cap analog. The standard deviations from three experiments are shown. (F) Translation of Kozak sequence driven *Renilla* luciferase mRNA, M1-5'UTR driven *Renilla* luciferase mRNA, and U2 snRNA + M1-5'UTR driven *Renilla* luciferase mRNA in HeLa lysate in the presence or absence of 1 mM m^7G cap analog. RNAs are capped at the 5'-end with m^7G and have a 100 nt long random UTR at the 3'-end. In each case, the RLU with the cap analog was normalized to the absence of cap analog arbitrarily set as 100%.

Supplemental Figure 6. PABP1 binding to the M1-5'UTR and M1-5'UTR Control RNAs and additional RT-qPCR analysis. (A) Sequence of the M1-5'UTR RNA and the M1-5'UTR control RNA. The M1-5'UTR control RNA is the complement counterpart to the M1-5'UTR sequence. Both sequences contain a guanosine at the 5'-end to improve T7 transcription of RNAs. (B) Anisotropy assay to determine the binding affinity of PABP1 for the M1-5'UTR and the M1-5'UTR control RNAs. The final concentration of the RNAs was 1 nM, and the final concentration of PABP1 was increased from 0 to 5 μM. The change in anisotropy is shown on the y-axis. The error bars represent the standard deviation from three independent experiments.

Supplemental Figure 7. PABP1 pulldown from IAV-infected cells enriches for viral 5'UTR RNAs. (A) Results of qPCR comparing the enrichment of RNA fragments from the 5'-end relative to fragments from the middle of IAV mRNAs. The data was normalized relative to the tubulin mRNA fragments from the 5'-end over middle arbitrarily set to 1 and the error was propagated for all conditions. (B) Results of RT-qPCR comparing the enrichment of RNA fragments from the 5'-end relative to fragments from the 3'-end of IAV mRNAs. The data was normalized relative to the actin mRNA fragments from the 5'-end over 3'-end arbitrarily set to 1 and the error was propagated for all conditions. (C) Results of qPCR comparing the enrichment of RNA fragments from the 5'-end relative to fragments from the 3'-end of IAV mRNAs. The data was normalized relative to the tubulin mRNA fragments from the 5'-end over 3'-end arbitrarily set to 1 and the error was propagated for all conditions. The cells were infected with A/Puerto Rico/8/34 (H1N1). The standard deviations from three biological

replicates are shown. $P < 0.05$ is denoted with one asterisk, $P < 0.01$ is denoted with two asterisks, $P < 0.001$ is denoted with three asterisks, and $P < 0.0001$ is denoted with four asterisks.

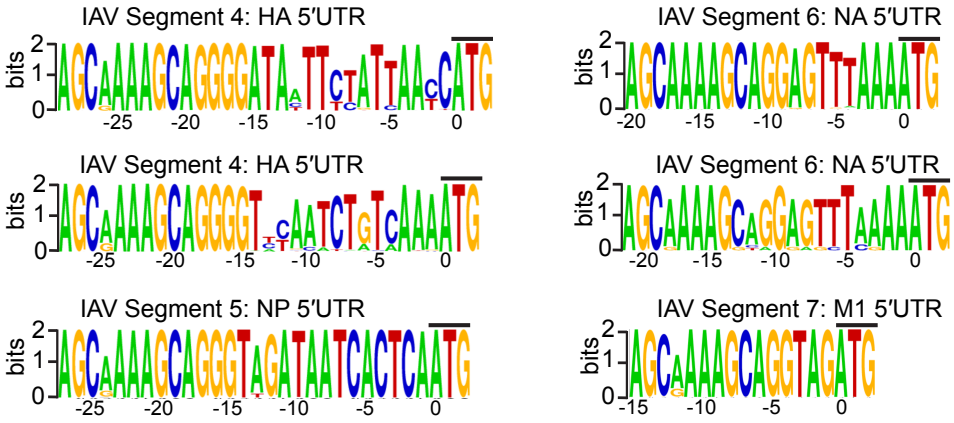

Supplemental Figure 1

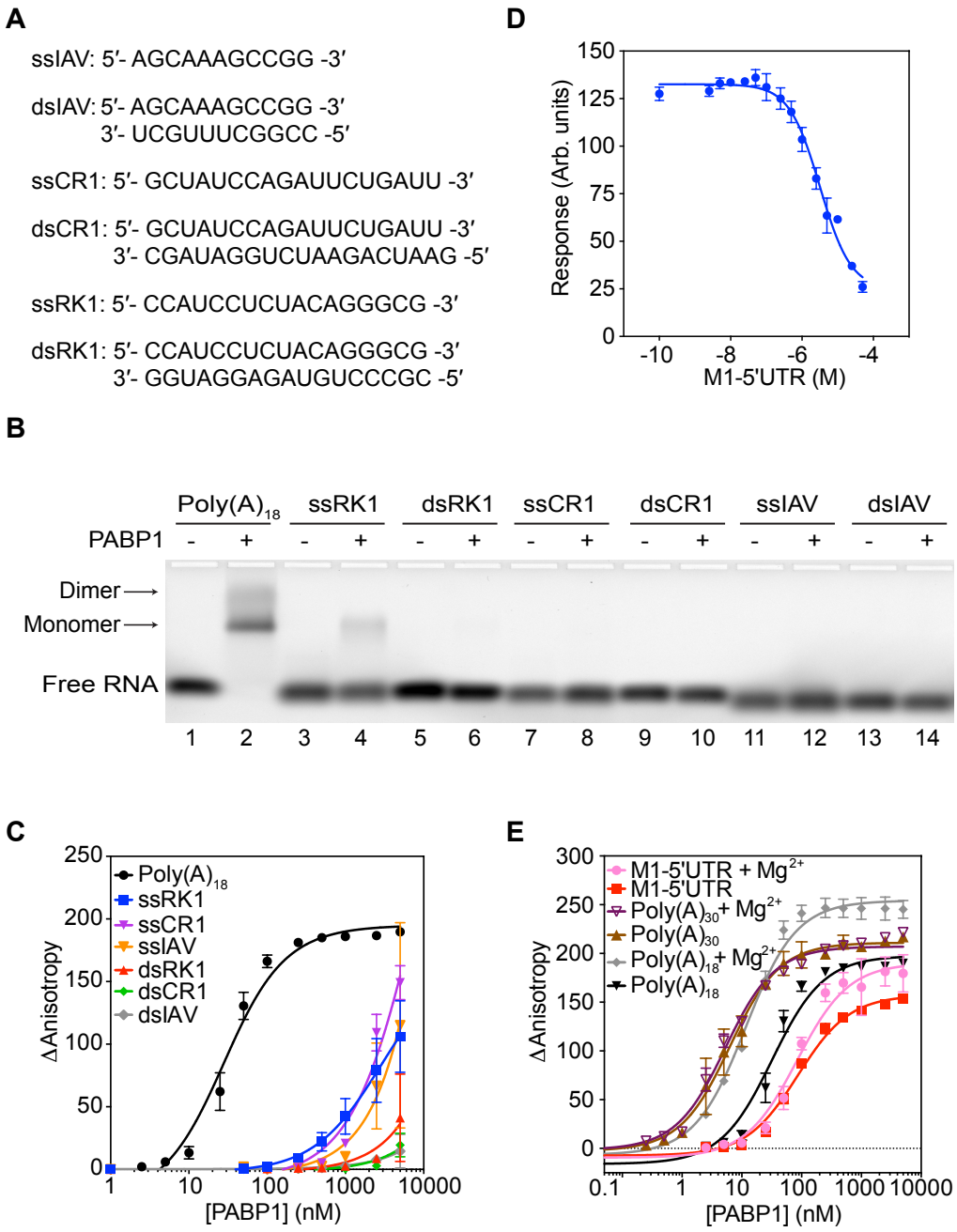

Supplemental Figure 2

A

A/Puerto Rico/8/34 (H1N1)

PB2: 5′- GAGCGAAAGCAGGUCAAUUAUAUUCAAU -3′
PB1: 5′- GAGCGAAAGCAGGCAAACCAUUUGA -3′
PA: 5′- GAGCGAAAGCAGGUACUGAUCCAAA -3′
HA: 5′- GAGCAAAAGCAGGGGAAAAUAAAAACAACCAAA -3′
NP: 5′- GAGCAAAAGCAGGGUAGAUAAUCACUCACUGAGUGACAUCAAAAUC -3′
NA: 5′- GAGCGAAAGCAGGAGUUUAAA -3′
M1: 5′- GAGCGAAAGCAGGUAGAUAUUGAAAG -3′
NS: 5′- GAGCAAAAGCAGGGUGACAAAAACAUA -3′

B

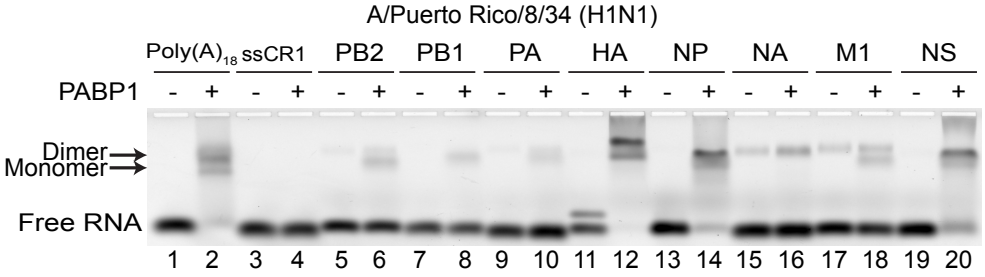

C

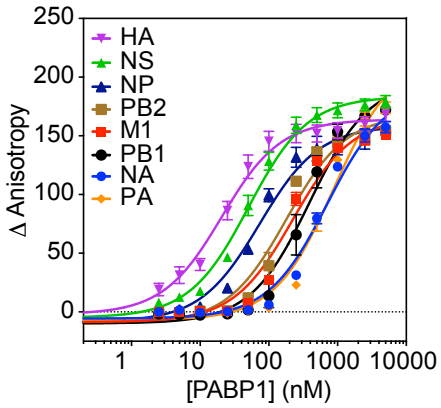

Supplemental Figure 3

A

A/Udorn/307/1972 (H3N2)

PB2: 5′- GAGCAAAAGCAGGUCAAUUAUAUUCAAU -3′
PB1: 5′- GAGCGAAAGCAGGCAAACCAUUUGA -3′
PA: 5′- GAGCAAAAGCAGGUACUGAUUCGAG -3′
HA: 5′- GAGCAAAAGCAGGGGAUAAUUCUAUUAACC -3′
NP: 5′- GAGCAAAAGCAGGGUUAAUAAUCACUCACUGAGUGACAUCAAAAUC -3′
NA: 5′- GAGCAAAAGCAGGAGUGAAG -3′
M1: 5′- GAGCAAAAGCAGGUAGAUAUUGAAAG -3′
NS: 5′- GAGCAAAAGCAGGGUGACAAAGACAUA -3′

B

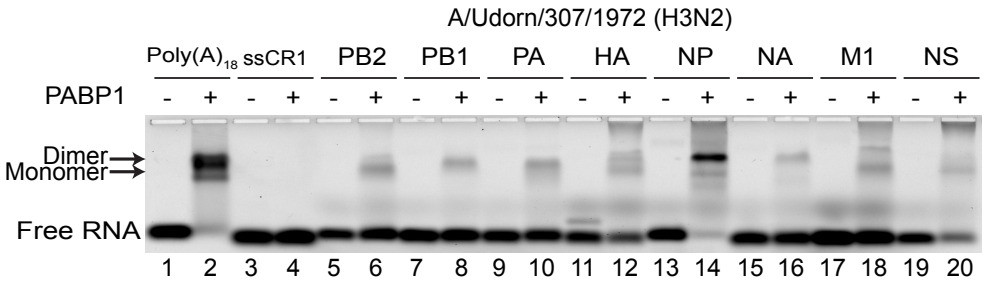

C

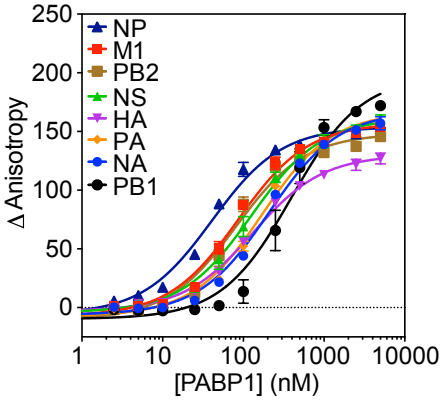

Supplemental Figure 4

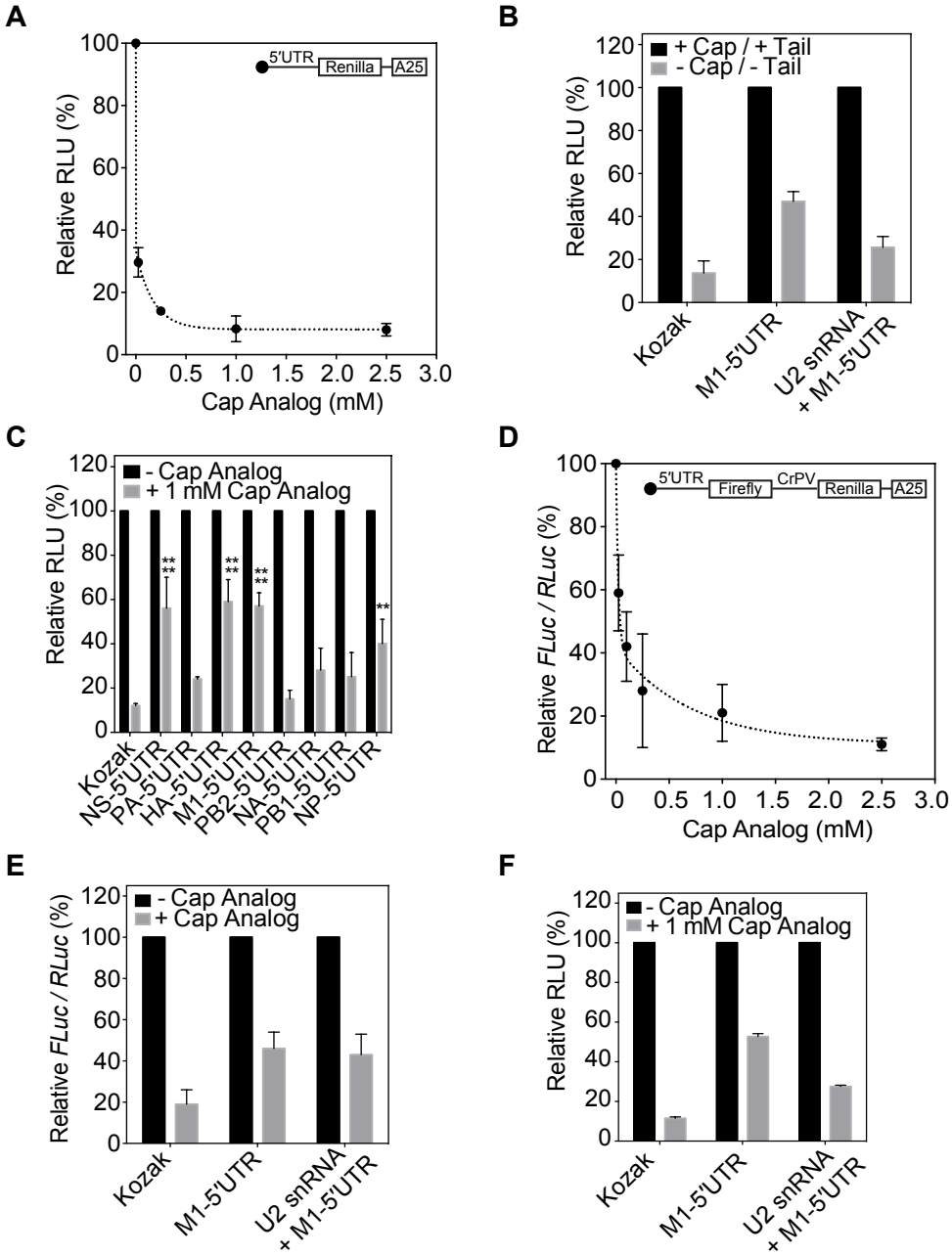

Supplemental Figure 5

A

M1 5′UTR: 5′- G A G C A A A A G C A G G U A G A U A U U G A A A G-3′
M1 5′UTR Control: 5′- G U C G U U U U C G U C C A U C U A U A A C U U U C-3′

B

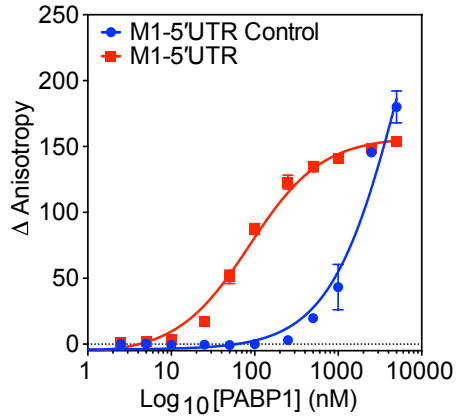

Supplemental Figure 6

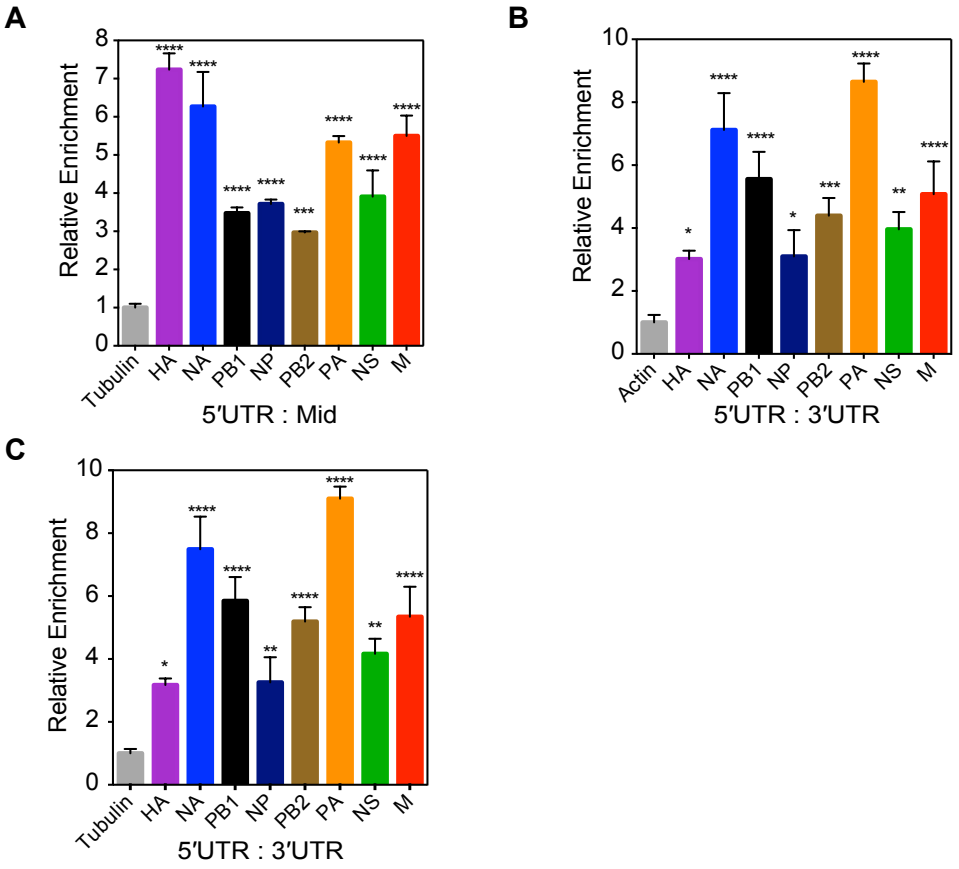

Supplemental Figure 7

Supplemental Table 1: Equilibrium Dissociation Constants (K_D) for PABP1 binding to the model IAV 5'UTR RNA

Sequence Name	Length (nt)	Sequence	K_D
U2 snRNA + M1-5'UTR	38	5'- GAUCGCUUCUCGCAGCAAAAGCAGGUAGAUAUUGAAAG -3'	106 nM ± 21 nM
U2 snRNA	13	5'- GAUCGCUUCUCGC -3'	1519 nM ± 720 nM
M1-5'UTR	26	5'- GAGCAAAAGCAGGUAGAUAUUGAAAG -3'	86 nM ± 7 nM
$Poly(A)_{18}$	18	5'-UAAAAAAAAAAAAAAAAA-3'	31 nM ± 4 nM
$Poly(A)_{30}$	33	5'-GGGAAAAAAAAAAAAAAAAAAAAAAAAAAAAA-3'	5 nM ± 0.5 nM

Supplemental Table 2: Equilibrium Dissociation Constants (K_D) for PABP1 binding to short control RNAs

Sequence Name	Length (nt)	Sequence	K_D
ssIAV	12	5'- AGCAAAAGCCGG -3'	No Binding
dsIAV	12	5'- AGCAAAAGCAGG -3' 3'- UCGUUUUCGUCC -5'	No Binding
ssCR1	18	5'- GCUAUCCAGAUUCUGAUU -3'	9.7 μM ± 4.6 μM
dsCR1	19	5'- GCUAUCCAGAUUCUGAUU -3' 3'- CGAUAGGUCUAAGACUAAG -5'	No Binding
ssRK1	16	5'- CCAUCCUCUACAGGCG -3'	3.0 μM ± 1.5 μM
dsRK1	16	5'- CCAUCCUCUACAGGCG -3' 3'- GGUAGGAGAUGUCCGC -5'	No Binding

* No binding refers to calculated K_D values greater than 10 μM.

Supplemental Table 3: Equilibrium Dissociation Constants (K_D) for PABP1 binding to the eight 5'UTR RNA of A/WSN/1933 (H1N1) IAV.

Sequence Name	Length (nt)	A/WSN/1933 (H1N1) 5'UTR Sequence	K_D
PB2 5'UTR	28	5'- GAGCGAAAGCAGGUCAAUUAUAUUCAAU -3'	181 nM ± 26 nM
PB1 5'UTR	25	5'- GAGCGAAAGCAGGCAAACCAUUUGA -3'	394 nM ± 52 nM
PA 5'UTR	25	5'- GAGCGAAAGCAGGUACUGAUUCAAA -3'	395 nM ± 44 nM
HA 5'UTR	33	5'- GAGCAAAAGCAGGGGAAAAUAAAAACAACCAAA -3'	20 nM ± 2 nM
NP 5'UTR	46	5'- GAGCAAAAGCAGGGUAGAUAAUCACUCACAGAGUGACAUCGAAAUC -3'	126 nM ± 14 nM
NA 5'UTR	21	5'- GAGCGAAAGCAGGAGUUUAA -3'	1004 nM ± 122 nM
M1 5'UTR	26	5'- GAGCAAAAGCAGGUAGAUAUUGAAAG -3'	86 nM ± 7 nM
NS 5'UTR	27	5'- GAGCAAAAGCAGGGUGACAAAGACAUA -3'	126 nM ± 9 nM

Supplemental Table 4: Equilibrium Dissociation Constants (K_D) for PABP1 binding to the eight 5'UTR RNA of A/Puerto Rico/8/34 (H1N1) IAV.

Sequence Name	Length (nt)	A/Puerto Rico/8/34 (H1N1) 5'UTR Sequence	K_D
PB2 5'UTR	28	5'- GAGCGAAAGCAGGUCAAUUAUAUUCAAU -3'	181 nM ± 26 nM
PB1 5'UTR	25	5'- GAGCGAAAGCAGGCAAACCAUUUGA -3'	394 nM ± 53 nM
PA 5'UTR	25	5'- GAGCGAAAGCAGGUACUGAUCCAAA -3'	883 nM ± 114 nM
HA 5'UTR	33	5'- GAGCAAAAGCAGGGGAAAAUAAAAACAACCAAA -3'	20 nM ± 2 nM
NP 5'UTR	46	5'- GAGCAAAAGCAGGGUAGAUAAUCACUCACUGAGUGACAUCAAAAUC -3'	73 nM ± 8 nM
NA 5'UTR	21	5'- GAGCGAAAGCAGGAGUUUAAA -3'	711 nM ± 83 nM
M1 5'UTR	26	5'- GAGCGAAAGCAGGUAGAUAUUGAAAG -3'	224 nM ± 31 nM
NS 5'UTR	27	5'- GAGCAAAAGCAGGGUGACAAAAACAUA -3'	50 nM ± 4 nM

Supplemental Table 5: Equilibrium Dissociation Constants (K_D) for PABP1 binding to the eight 5'UTR RNA of A/Udorn/307/1972 (H3N2) IAV.

Sequence Name	Length (nt)	A/Udorn/307/1972 (H3N2) 5'UTR Sequence	K_D
PB2 5'UTR	28	5'- GAGCAAAAGCAGGUCAAUUAUAUUCAAU -3'	81 nM ± 9 nM
PB1 5'UTR	25	5'- GAGCGAAAGCAGGCAAACCAUUUGA -3'	394 nM ± 53 nM
PA 5'UTR	25	5'- GAGCAAAAGCAGGUACUGAUUCGAG -3'	171 nM ± 13 nM
HA 5'UTR	30	5'- GAGCAAAAGCAGGGGAUAAUUCUAUUAACC -3'	131 nM ± 7 nM
NP 5'UTR	46	5'- GAGCAAAAGCAGGGUUAAUAAUCACUCACUGAGUGACAUCAAAAUC -3'	40 nM ± 3 nM
NA 5'UTR	20	5'- GAGCAAAAGCAGGAGUGAAG -3'	205 nM ± 14 nM
M1 5'UTR	26	5'- GAGCAAAAGCAGGUAGAUAUUGAAAG -3'	86 nM ± 7 nM
NS 5'UTR	27	5'- GAGCAAAAGCAGGGUGACAAAGACAUA -3'	126 nM ± 9 nM